Step Dance on a Pentagon: Copper(I) and Copper(I)−Tungsten(0) Triphospholyl Triphenylphosphane Complexes†

Frank W. Heinemann, Matthias Zeller,‡ and Ulrich Zenneck*

Institut für Anorganische Chemie, Universität Erlangen-Nürnberg, Egerlandstrasse 1, 91058 Erlangen, Germany

Received August 8, 2003

[(3,5-di-*tert*-butyl-1,2,4-triphospholyl)Cu(PPh_3)] (**3**) is, in contrast to the related dimeric complex [(3,5-di-*tert*-butyl-1,2,4-triphospholyl)Cu(PMe_3)$_2$]$_2$, monomeric and highly fluxional in solution. **3** is synthesized from the corresponding trimethylstannyl 1,2,4-triphosphole **1a** and [ClCu(PPh_3)]$_4$. Evidence for a three-sided rearrangement process between different molecular structures in solution could be obtained from dynamic ^{31}P NMR spectroscopy. An η^5-π coordination mode (**3a**) of the copper ion is preferred at room temperature. The equilibrium shifts to the two spectroscopically distinguishable, but almost isoenergetic, σ complexes **3b** and **3c** at low temperature, which interconvert with the activation barrier $\Delta G^{\ddagger} = 37$ kJ/mol. The σ-donor orbitals of the triphospholyl ligand are believed to be an sp^3 hybrid P orbital in the case of **3b** and an sp^2 P lone pair for **3c**. The reaction of **3** with [(THF)W(CO)$_5$] leads to the binuclear CuW complex **4** and the trinuclear W_2Cu complex **5** with σ-phosphorus-coordinated W(CO)$_5$ moieties. **5** bears an additional η^5-π coordinated W(CO)$_3$ unit and a unique W−Cu−P bridge, as established by X-ray crystallography. Both complexes are fluxional in solution, and the activation barriers of their rearrangement processes have been established.

Introduction

Phosphorus atoms can be incorporated in unsaturated heterocycles to replace CR fragments as isovalent and isolobal building blocks, which results in the formation of numerous organophosphorus and organometallic phosphorus compounds in which the phosphorus atom can often be viewed as a close relative of the element carbon.[1] On the other hand, each phosphorus atom supplies a lone pair to the ring molecules, causes a decrease of the frontier π-orbital energies, and expands its ring size with respect to the pure carbon ring analogues. All three aspects modify the ligand properties of such heterocycles; however, the differences are not dominant for compounds having less than half of the CR fragments substituted by phosphorus atoms. That changes significantly when the number of ring phosphorus atoms equals or exceeds that of the carbon atoms as in the case of 1,3,5-triphosphinine,[1b−d] 1,2,4-triphospholyl,[3−7] or 1,3-diphosphete[2] ligands. In these examples, the heterocycles cannot be viewed as simple analogues of their carbocyclic parent compounds any longer.

Unlike cyclopentadienyl (Cp) derivatives, not only are the ligand properties of 1,2,4-triphospholyl ligands therefore governed by the delocalized π-system but also the phosphorus lone pairs play a comparably active role. In principle, they can be utilized independently from the π-electrons as phosphine-like σ-donor functions toward metal centers. On the other hand, they allow intra- and intermolecular σ-/π-rearrangement processes with low activation barriers. The 1,5-sigmatropic shift of the tin atoms of triorganylstannyl-1,2,4-triphosphole derivatives (**1**), for example, requires an activation energy of only 31 kJ mol^{-1},[3] and a related rearrangement for bis(1,2,4-triphospholyl)mercury occurs even in the solid state.[4] Novel structural features have been observed for the molecular structures of 1,2,4-triphospholyl complexes of Ni, Pd, and Pt, which are not known for Cp ligands. This includes a reversible equilibrium

* To whom correspondence should be addressed. Fax: Int. code +(9131)852-7367. E-mail: zenneck@chemie.uni-erlangen.de.

† Dedicated in honor of Professor Dr. Otto Scherer on the occasion of his 70th birthday.

‡ Current address: Youngstown State University, Department of Chemistry, 1 University Plaza, Youngstown, OH 44555-3663. E-mail: mzeller@cc.ysu.edu.

(1) (a) Dillon, K. B.; Mathey, F.; Nixon, J. F. *Phosphorus, The Carbon Copy*; Wiley: Chichester, U.K., 1998. (b) Vlaar, M. J. M.; Ehlers, A. W.; Schakel, M.; Clendenning, S. B.; Nixon, J. F.; Lutz, M.; Spek, A. L.; Lammertsma, K. *Angew. Chem., Int. Ed.* **2001**, *40*(23), 4412−4415. (c) Peters, C.; Disteldorf, H.; Fuchs, E.; Werner, S.; Stutzmann, S.; Bruckmann, J.; Kruger, C.; Binger, P.; Heydt, H.; Regitz, M. *Eur. J. Org. Chem.* **2001**, *18*, 3425−3435. (d) Hofmann, M.; Schleyer, P. v. R.; Regitz, M. *Eur. J. Org. Chem.* **1999**, *12*, 3291−3303.

(2) Topf, C.; Clark, T.; Heinemann, F. W.; Hennemann, M.; Kummer, S.; Pritzkow, H.; Zenneck, U. *Angew. Chem.* **2002**, *114*, 4221−4226; *Angew. Chem., Int. Ed.* **2002**, *41*, 4047−4052.

(3) Elvers, A.; Heinemann, F. W.; Wrackmeyer, B.; Zenneck, U. *Chem. Eur. J.* **1999**, *5*(11), 3143−3153.

(4) Al-Ktaifani, M. M.; Bauer, W.; Bergsträsser, U.; Breit, B.; Francis, M. D.; Heinemann, F. W.; Hitchcock, P. B.; Mack, A.; Nixon, J. F.; Pritzkow, H.; Regitz, M.; Zeller, M.; Zenneck, U. *Chem. Eur. J.* **2002**, *8*, 2622−2633.

(5) Heinemann, F. W.; Pritzkow, H.; Zeller, M.; Zenneck, U. *Organometallics* **2000**, *19*, 4283−4288.

(6) Heinemann, F. W.; Hofmann, M.; Zenneck, U. *J. Organomet. Chem.* **2002**, *643−644*, 357−362.

(7) Clark, T.; Heinemann, F. W.; Hennemann, M.; Zeller, M.; Zenneck, U. *Angew. Chem.* **2000**, *112*, 2174−2178; *Angew. Chem., Int. Ed.* **2000**, *39*, 2087−2091.

10.1021/om030570i CCC: $27.50
Publication on Web 03/19/2004

Scheme 1

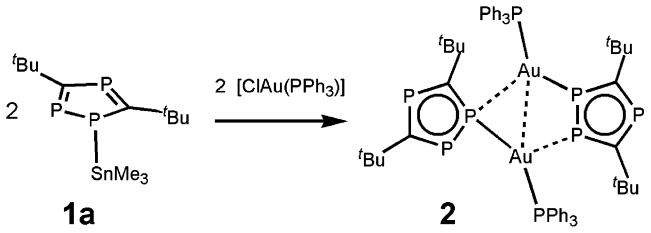

Scheme 2

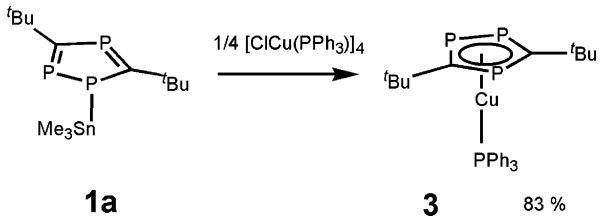

between a Ni σ-complex dimer and its mononuclear π-derivative.[5] The removal of only one phosphorus atom from the triphospholyl ring skips these effects almost completely. Neither triorganylstannyl-1,3-diphospholes nor (η^5-1,3-diphospholyl)copper triphenylphosphine shows any sign of dynamic effects at ambient temperature.[8]

With the aim of learning more about the specific ligand properties of the 3,5-di-*tert*-butyl-1,2,4-triphospholyl ligand, we investigated its complex chemistry with respect to the coinage metals gold and copper. In a first communication on the gold complexes, we reported about highly dynamic mixtures of interchanging isomers of [(3,5-di-*tert*-butyl-1,2,4-triphospholyl)Au(PPh_3)] in solution. In the solid state we observe the extremely asymmetric σ-complex dimer [(3,5-di-*tert*-butyl-1,2,4-triphospholyl)Au(PPh_3)]$_2$ (**2**) with a remarkable range of different metal−triphospholyl interactions[6] (Scheme 1).

If the PPh_3 ligand is just replaced by PEt_3, a completely different dinuclear species, [{Au(PEt_3)$_2$}{Au(3,5-di-*tert*-butyl-1,2,4-triphospholyl)$_2$}], is observed in the solid state.[9] These results indicate shallow energetic minima for 1,2,4-triphospholyl gold species. Packing might influence the molecular structures in the solid state, and several monomer−dimer and monomer−monomer equilibria exist for **2** in solution which are too complex to be analyzed unambiguously by NMR techniques. Nixon and co-workers reported about two static binuclear (μ,σ-3,5-di-*tert*-butyl-1,2,4-triphospholyl)$_n$$Cu_2$($PMe_3$)$_4$ (n = 1, 2) complexes,[9] whose $L_2M(\mu,\sigma$-1,2,4-triphospholyl)ML_2 moieties are isostructural with the dimeric Ni(II) species [(μ,σ-3,5-di-*tert*-butyl-1,2,4-triphospholyl)$_2$$Ni_2(NO)_2$($PPh_3$)$_2$].[5]

In this paper we report on our results on the preparation and dynamic NMR spectroscopy of a monomeric copper analogue of **2**, [(3,5-di-*tert*-butyl-1,2,4-triphospholyl)Cu(PPh_3)] (**3**). With the aim of reducing the highly dynamic effects of **3** in solution by blocking the phosphorus lone pairs, we utilized it as a ligand of tungsten carbonyl complexes. To our surprise, the resulting di- and trinuclear bimetallic CuW complexes are as fluxional as mononuclear **3**.

Results

The target complex [(3,5-di-*tert*-butyl-1,2,4-triphospholyl)Cu(PPh_3)] (**3**) is formed in good yield through the reaction of 1-Me_3Sn-3,5-di-*tert*-butyl-1,2,4-triphosphole (**1a**) with the tetrameric copper complex [ClCu(PPh_3)]$_4$ (Scheme 2).

The triphospholyl complex **3** forms orange to yellow microcrystalline solids. All attempts to prepare single-crystalline material of **3** failed up to now. Room-temperature ^{1}H NMR spectra of **3** exhibit phenyl multiplets and one sharp *tert*-butyl resonance. The ^{13}C NMR signals of the triphospholyl ligand are split by ^{31}P coupling into pseudotriplets. These findings are in line with both a symmetrical η^5-coordinated or a highly fluxional η^1-coordinated triphospholyl ligand. The ^{31}P{^{1}H} NMR spectrum consists of three signals at 204, 188, and 8 ppm, respectively. Unlike ^{1}H and ^{13}C NMR, the room-temperature ^{31}P{^{1}H} NMR signals of **3** indicate dynamic processes on the time scale of NMR spectroscopy, as they are significantly broadened. Variable-temperature ^{31}P{^{1}H} NMR measurements proved this assumption. Slow-exchange-limit spectra of two different η^1 isomers are observable at low temperatures (Figure 1).

When the sample is warmed to +48 °C, the general appearance of the spectrum remains constant, but the line width decreases and a $^2J_{P,P}$ coupling between the two types of ring phosphorus atoms becomes visible. Its value of 55 Hz gives a hint of the significant participation of a η^5 coordination mode (**3a**) with a delocalized π system at elevated temperatures. The position of the two triphospholyl signals around 200 ppm are compatible with this assumption as well. In contrast to that, the room-temperature observations in solution for the known 1,2,4-triphospholyl Au(I) and Cu(I) complexes strongly favor η^1-bonding modes of the heterocycle.[6,9]

When the ^{31}P NMR sample is cooled, the line widths of the signals increase and reach a maximum around −10 °C. At lower temperatures, new signals grow in and those which are observable at the high-temperature lose intensity, move slightly, and sharpen at the same time. At −70 °C they are no longer broadened and, as expected for a pure η^5-bonding mode, the doublet and triplet signals of an AB_2 partial spin system are observed for the ring phosphorus atoms ($^2J_{P,P}$ = 49.6 Hz) while the PPh_3 signal remains unsplit.

Around −30 °C a new set of resonances arises, which form an AB_2X spin system as well. The A and B signals of this set are separated by almost 100 ppm, and the A resonance is shifted to a remarkably low field value (277 ppm). Related chemical shifts are indicative of phosphaalkenes. A fluxional η^1-coordination of the copper atom would be in line with the data. As proven for triorganylstannyl triphospholes (**1**), a fast 1,5-sigmatropic rearrangement of the metal can explain this part of the observations. If so, the AB_2X spin system should be transformed into an ABCX system at very low temperature. This is indeed the case; however, two ABCX sets of the same intensity are observed at −90 °C and the AB_2X spin system of η^5 complex **3a** is present at this temperature in only very small intensity. The two ABCX spin system signals are relatively broad; thus, only one $^1J_{PP}$ coupling of approximately 357 Hz is

(8) Zeller, M. Ph.D. Thesis, University of Erlangen-Nürnberg, 2000.
(9) Al-Ktaifani, M. M.; Hitchcock, P. B.; Nixon, J. F. *J. Organomet. Chem.* **2003**, *665*, 101−106.

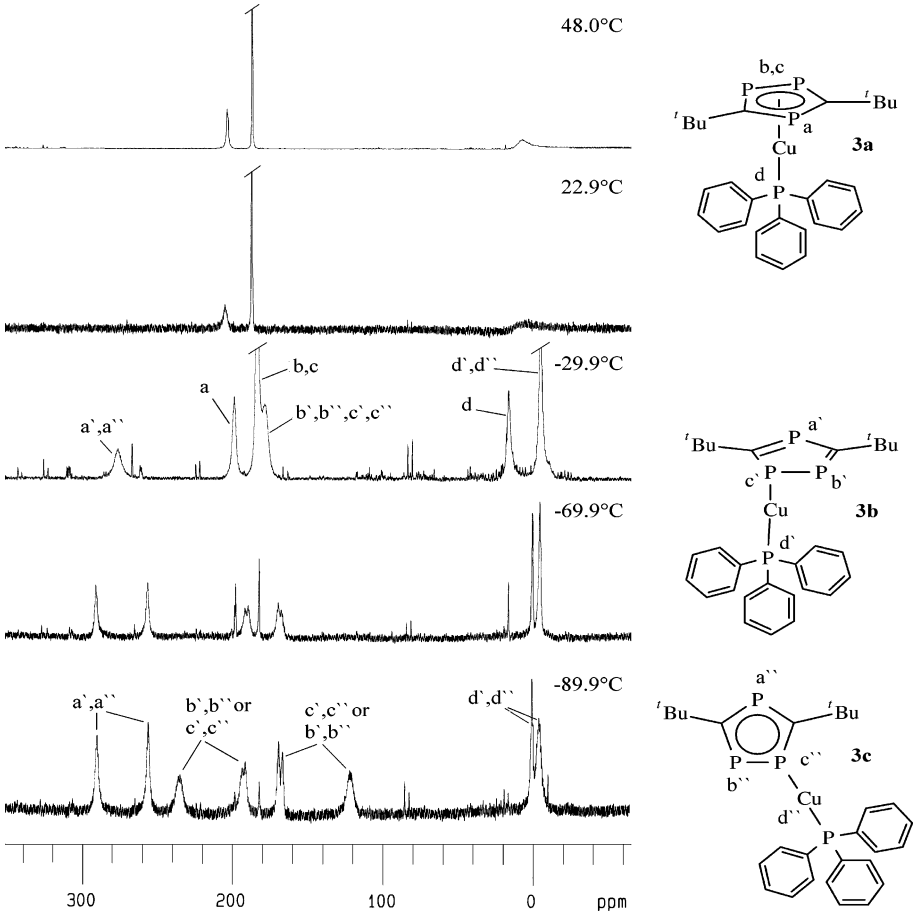

Figure 1. Variable-temperature $^{31}P\{^1H\}$ NMR spectra of **3** (161.7 MHz, [D_8]toluene).

resolved. Two of the signals arising from the loss of equivalence of the two neighboring P ring atoms are not detectable between −50 and −70 °C, a hint of an additional dynamic process.

This complicated NMR spectroscopic behavior could be explained principally by the formation of an asymmetric dimer at low temperatures, as observed for **1**. A symmetric dimer such as [(μ,σ-3,5-di-*tert*-butyl-1,2,4-triphospholyl)$_2$Cu$_2$(PMe$_3$)$_4$] is definitely incompatible with the spectra.[9] On the basis of the observed coalescence phenomena, such a dimer would have to be highly dynamic, and two independent rearrangement processes with different activation barriers are required to fit to the dynamic spectra.

A low-temperature equilibrium between two different but almost isoenergetic monomeric complexes is the second possibility. The experimental findings can be more easily and completely explained by an NMR spectroscopic slow rearrangement between the η^5 complex **3a** and the two σ-bonded isomers **3b** and **3c** and a fast equilibrium between the σ complexes. **3b** is characterized by an η^1 σ-sp^3(P)−Cu interaction and a localized ring π system. An sp^2(P) lone pair binds to the copper atom of **3c**, and a free delocalized π^6 system is formed by the ring elements of the coordinated triphospholyl ligand, as shown in Scheme 3.

The ligand−metal bonding mode of isomer **3b** is believed to be closely related to that of triorganylstannyl triphospholes **1**.[3,8] The η^1 coordination of cyclopentadienyl ligands, when bonded to gold(I), is an alternative model.[10] The combination of a lone pair coordination and a free delocalized π^6 system as in **3c** is impossible for cyclopentadienyl ligands but requires a phosphorus atom or another element with a lone pair as a ring element. Examples of the postulated structure type **3c** have been characterized for some triphospholyl Pt and Pd[11] complexes. Dimeric Ni(II) and Cu(II) triphospholyl complexes share the σ M−L interaction and the delocalized π system.[5,9]

The kinetic and thermodynamic parameters, which can be extracted from the observed coalescence temperatures and the relative concentrations of the three isomers **3a**−**c**, give hints in the same direction (Scheme 3). The activation energy for the 1,5-sigmatropic shift of the copper atom of **3b** can be estimated at 31(2) kJ/mol (coalescence of ^{31}P signals at 235 and 122 ppm at −70 °C).[12] An almost identical value was determined for the respective process of triorganylstannyl triphospholes **1**.[3] For the more complex rearrangement equilibrium between **3b** and **3c**, which is associated with localization and delocalization of the π electrons and the rehybridization of the metal bonding P-orbitals from sp^3 into sp^2, the activation barrier is estimated to be 37(2) kJ/mol (coalescence of ^{31}P signal pairs at 292/267 and

(10) Werner, H.; Otto, H.; Ngo-Khac, T.; Burschka, C. *J. Organomet. Chem.* **1984**, *262*, 123−136.
(11) (a) Bartsch, R.; Carmichael, D.; Hitchcock, P. B.; Meidine, M. F.; Nixon, J. F.; Sillet, G. J. D. *J. Chem. Soc., Chem. Commun.* **1988**, 1615−1617. (b) Nixon, J. F.; Sillet, G. J. D. *J. Organomet. Chem.* **1993**, *461*, 237−245.
(12) Friebolin, H. *Ein- und Zweidimensionale NMR-Spektroskopie und ihre Anwendungen in der Chemie*, 2nd ed.; Georg Thieme Verlag: Stuttgart, Germany, 1983.

Scheme 3

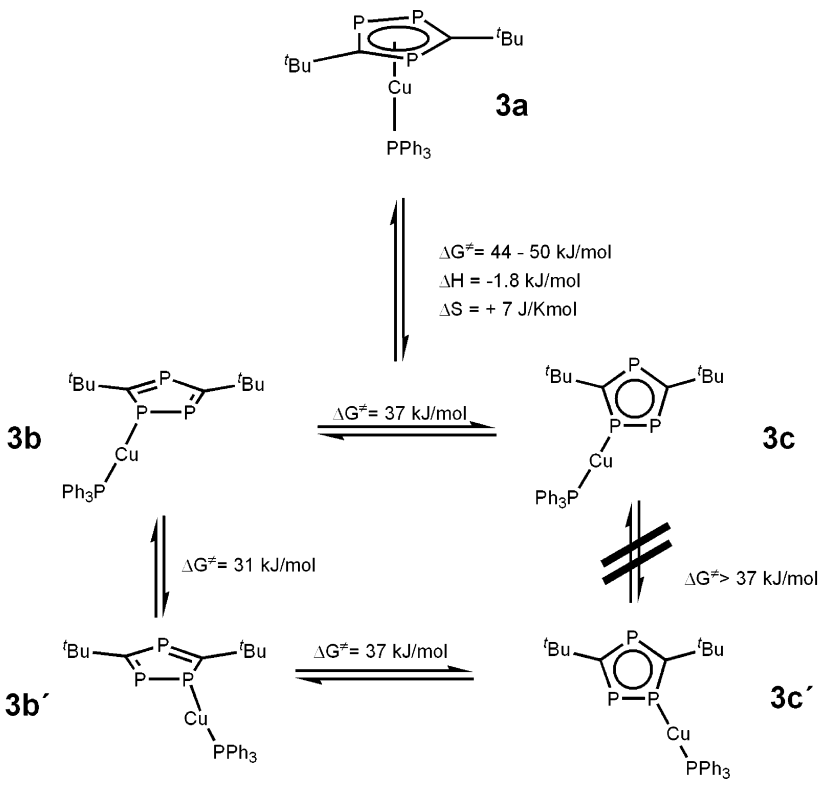

193/168 ppm around −50 °C). The observation of a higher activation barrier for this process seems to make sense; however, such an equilibrium is a rare case, as we did not find comparable observations in the literature. From the temperature dependence of the relative concentration of **3a** versus **3b** plus **3c** we can estimate the thermodynamic parameters for the $\eta^5 \leftrightarrow \eta^1$ rearrangements **3a** versus interchanging **3b** and **3c**.[8]

Copper−Tungsten Triphospholyl Complexes. As we failed to obtain crystals of suitable quality, no X-ray structural analysis and thus no direct proof of the postulated molecular structures **3a−c** was possible. With the aim of increasing the crystallization properties and reducing the complexity of the dynamic NMR spectra by blocking one phosphorus lone pair at the minimum, we modified complex **3** by complexation to a suitable metal carbonyl fragment. When **3** is reacted with in situ generated [(THF)W(CO)$_5$] in THF, the binuclear CuW complex **4** and trinuclear W_2Cu complex **5** are formed. Chromatography on water-deactivated silica and recrystallization from CH_2Cl_2/*n*-hexane leads to their separation in single-crystalline form (Scheme 4)

Scheme 4

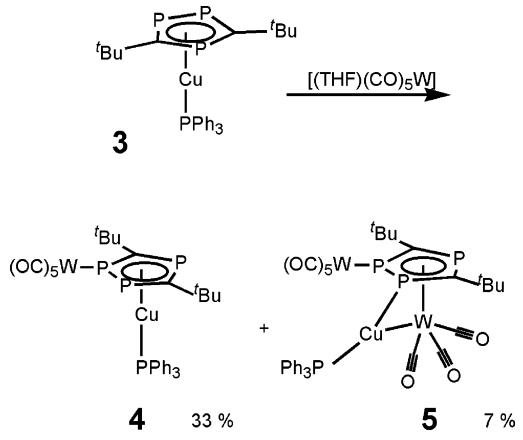

Bright yellow **4** crystallizes in the monoclinic space group $P2_1/n$ with approximately 0.8 equiv of CH_2Cl_2 per complex molecule. The solvent molecules are disordered in channels parallel to the *b* axis of the elemental cell. A pentacarbonyltungsten fragment is attached to one of the two adjacent phosphorus atoms of the triphospholyl ring, and the copper atom is in bonding contact with all five ring atoms as proposed for **3a**. This represents 18-valence-electron (VE) bonding situations for both metal atoms (Figure 2 and Tables 1 and 3).

Due to the influence of the three phosphorus atoms and the attached W(CO)$_5$ moiety, there are some differences between corresponding molecular structure data of the tungsten-complexed [(1,2,4-triphospholyl)-Cu(PPh$_3$)] compound **4** and its [CpCu(PR$_3$)] analogues. The phosphine−Cu bond length P(4)−Cu(1) = 2.180(3) Å is elongated by 4.5 pm, and the distance between the Cu atom and the center of the planar ring ligand is shortened by 6 and 10 pm, respectively, with regard to the CpCu complexes [CpCu(PPh$_3$)] and [CpCu(PEt$_3$)].[13] In contrast to the Cp complexes, the angle between the two bond vectors of the Cu atom (Cu(1)−P(4) vs Cu(1)−center of the ring ligand) equals 170.3(2)° and thus deviates by nearly 10° from linearity. Almost the same deviation from the idealized rectangular arrangement is found for the angle between the vectors Cu(1)−P(4) and P(3)−W(1), 102.2(2)°. The increase of 12° with respect to 90° fits the observed deviation from a linear orientation of both ligands.

(13) (a) Cotton, F. A.; Takats, J. *J. Am. Chem. Soc.* **1970**, *92*, 2353−2358. (b) Delbaere, L. T. J.; McBride, D. W.; Ferguson, R. B. *Acta Crystallogr., Sect. B* **1970**, *26*, 515−521.

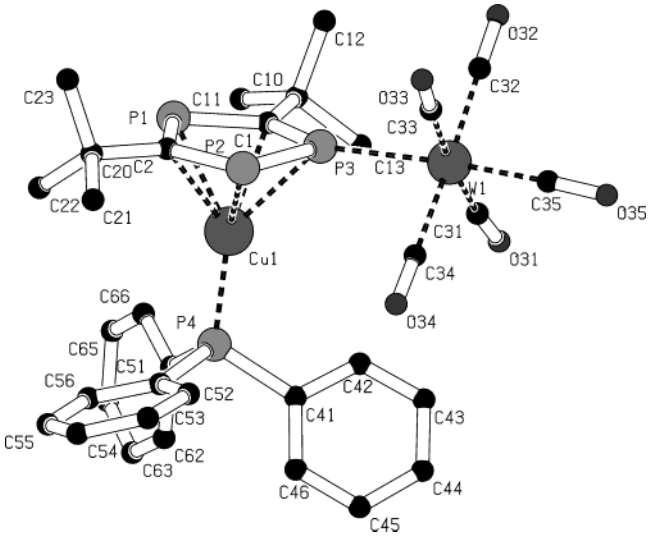

Figure 2. Molecular structure of **4** in the solid state. Hydrogen atoms are omitted for clarity.

Table 1. Selected Bond Lengths (Å) and Angles (deg) for 4

W−P(3)	2.532(2)	C(35)−O(35)	1.158(9)
P(3)−P(2)	2.113(3)	C(31)−O(31)	1.138(10)
P(2)−C(2)	1.751(8)	C(32)−O(32)	1.123(9)
C(2)−P(1)	1.754(8)	C(33)−O(33)	1.161(10)
P(1)−C(1)	1.788(8)	C(34)−O(34)	1.124(9)
C(1)−P(3)	1.740(8)	Cu−P(4)	2.180(3)
W−C(35)	1.987(10)	Cu−C(1)	2.274(8)
W−C(31)	2.010(11)	Cu−C(2)	2.277(8)
W−C(32)	2.027(10)	Cu−P(1)	2.417(3)
W−C(33)	2.004(11)	Cu−P(2)	2.473(3)
W−C(34)	2.077(10)	Cu−P(3)	2.438(3)
C(2)−P(1)−C(1)	100.1(4)	P(2)−C(2)−P(1)	121.8(5)
P(1)−C(1)−P(3)	118.0(5)	W−P(3)−C(1)	141.0(3)
C(1)−P(3)−P(2)	102.1(3)	W−P(3)−P(2)	116.9(1)
P(3)−P(2)−C(2)	97.8(3)		

Table 2. Selected Bond Length (Å) and Angles (deg) for 5

W(1)−Cu	2.646(2)	W(1)−C(32)	1.97(2)
Cu−P(4)	2.238(4)	W(1)−C(33)	1.97(2)
Cu−P(2)	2.390(4)	C(31)−O(31)	1.17(2)
W(2)−P(3)	2.498(4)	P(2)−W(1)	2.623(4)
P(3)−P(2)	2.138(5)	P(1)−W(1)	2.561(4)
P(2)−C(1)	1.82(2)	P(3)−W(1)	2.576(4)
C(1)−P(1)	1.73(2)	C(1)−W(1)	2.37(2)
P(1)−C(2)	1.81(2)	C(2)−W(1)	2.44(2)
C(2)−P(3)	1.75(2)	C(32)−O(32)	1.17(2)
W(1)−C(31)	1.96(2)	C(33)−O(33)	1.16(2)
W(1)−Cu−P(4)	154.3(2)	C(2)−P(3)−P(2)	102.6(6)
W(1)−Cu−P(2)	62.5(1)	P(3)−P(2)−C(1)	95.9(5)
P(2)−Cu−P(4)	143.1(2)	P(2)−C(1)−P(1)	122.7(8)
C(1)−P(1)−C(2)	100.0(7)	C(2)−P(3)−W(2)	140.9(6)
P(1)−C(2)−P(3)	118.3(9)	P(2)−P(3)−W(2)	115.9(2)

5 forms orange plates. The space group of the crystal is $P2_1/c$. Not only is the targeted σ-bonded $(CO)_5W$ fragment present but also an additional $W(CO)_3$ moiety completes the trinuclear complex **5**. Tungsten atom W(1) and the $(Ph_3P)Cu(1)$ moiety form a bridge to one of the two adjacent phosphorus atoms P(2) of the triphospholyl ring. Its neighbor P(3) binds the $W(2)(CO)_5$ fragment (Figure 3 and Tables 2 and 3). Both tungsten atoms, W(1) and W(2), exhibit 18-VE shells, but, as usual for trigonal coordinated coinage metals, the VE sum of Cu equals 16. To the best of our knowledge, the molecular structure of **5** is without precedence in copper complex chemistry; only a dimeric Pt−W triphospholyl complex shares some of its features.[14]

The 1,2,4-triphospholyl ligand of **5** is markedly distorted. The angle P(3)−P(2)−C(1) is reduced to only

Table 3. Crystal Data and Structure Refinement Details for 4 and 5

	4	**5**
empirical formula	$C_{33.8}H_{34.6}Cl_{1.6}CuO_5P_4W$	$C_{36}H_{33}CuO_8P_4W_2$
formula wt	948.80	1148.74
solvent	*n*-hexane/CH_2Cl_2	*n*-hexane/CH_2Cl_2
cryst habit	yellow needle	orange plate
temp, K	298(2)	220(2)
cryst syst	monoclinic	monoclinic
space group	$P2_1/n$	$P2_1/c$
unit cell dimens		
a, Å	15.598(6)	16.120(2)
b, Å	10.842(4)	10.727(2)
c, Å	24.242(13)	22.954(6)
α, deg	90	90
β, deg	92.72(4)	98.14(2)
γ, deg	90	90
V, Å^3	4095(3)	3929(2)
Z	4	4
calcd density, g/cm^3	1.539	1.942
abs coeff, mm^{-1}	3.622	6.588
F(000)	1870	2200
cryst size, mm	0.40 × 0.15 × 0.10	0.42 × 0.18 × 0.08
θ range for data collecn, deg	2.06−27.06	1.79−26.01
index ranges	$-19 \le h \le 19$ $-1 \le k \le 13$ $-1 \le l \le 31$	$-19 \le h \le 1$ $-13 \le k \le 1$ $-28 \le l \le 28$
no. of rflns collected	16 002	9531
no. of indep rflns	8949 (*R*(int) = 0.0657)	7713 (*R*(int) = 0.0841)
no. of rflns with $I > 2\sigma(I)$	2935	4950
completeness, % (to *θ*, deg)	99.6 (27.06)	99.9 (26.01)
abs cor	*ψ* scan	integration
max and min transmissn	0.168 and 0.118	0.556 and 0.280
no. of data/restraints/params	8949/5/424	7713/0/466
goodness of fit on F^2	0.678	1.056
final *R* indices ($I > 2\sigma(I)$)	R1 = 0.0466, wR2 = 0.0651	R1 = 0.0666, wR2 = 0.1419
R indices (all data)	R1 = 0.1812, wR2 = 0.0868	R1 = 0.1198, wR2 = 0.1671
largest diff peak and hole, e Å^{-3}	0.658 and −0.899	2.367 and −3.754

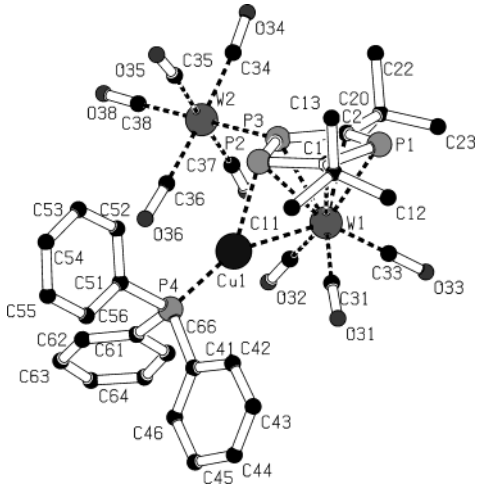

Figure 3. Molecular structure of **5** in the solid state. Hydrogen atoms are omitted for clarity.

(14) Bartsch, R.; Meidine, M. F.; Nixon, J. F.; Sillet, G. J. D. *J. Chem. Soc., Chem. Commun.* **1990**, 317−319.

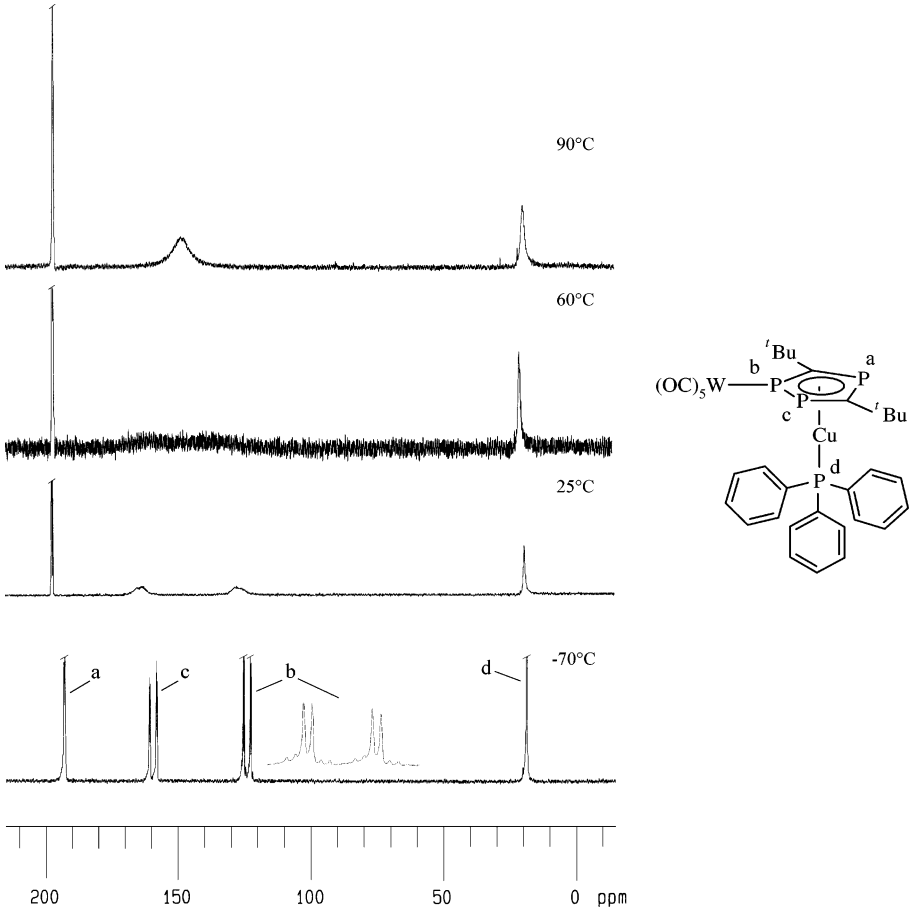

Figure 4. Variable-temperature $^{31}P\{^1H\}$ NMR spectra of **4** (161.7 MHz; 25 to −70 °C, CD_2Cl_2; 60 to 90 °C, $[D_8]$toluene).

95.9(5)°, and the intra-ring P−C bond lengths are alternating. The differences of adjacent P−C bond lengths of 5−8 pm are very close to those observed for the stannyl triphospholes **1**, which exhibits an unquestionable diene character in the solid state.[3] The ring distortion of **5**, however, is most probably caused by the asymmetrical coordination of Cu(1) and η^5-bonded W(1). The two bond distances W(1)−P(1) and W(1)−P(3) equal 2.561(4) and 2.576(4) Å, respectively, whereas the Cu(1)-bound P(2) enhances its distance to W(1) to significantly at 2.623(4) Å. The bond distance Cu(1)−W(1) is in the normal range observed for other Cu−W single bonds (2.646(2) Å).

In contrast to our expectations, both **4** and **5** are fluxional in solution. For **4** a 1,2-shift of the tungsten atom is observed by variable-temperature ^{31}P NMR spectroscopy (Figure 4).

At −70 °C the spectrum of **4** is well resolved, including ^{31}P and ^{183}W coupling patterns. The $^1J(^{183}W,^{31}P)$ coupling constant is 213 Hz, $^1J(^{31}P,^{31}P)$ is 424.5 Hz, and the two $^2J(^{31}P,^{31}P)$ coupling constants are 49.3 and 54.2 Hz, respectively. Around 60 °C the signals of the two adjacent phosphorus atoms coalesce and an activation barrier of 55.6(9) kJ/mol results for the 1,2-shift of the tungsten atom.[12] This value is remarkably small. Most studies on triphospholyl π-complexes with an additional metal fragment being bonded to a phosphorus lone pair do not mention dynamic effects. An exception are two metal pentacarbonyl complexes of triphosphaferrocene, [(η^5-Cp*)Fe(η^5-(3,5-di-*tert*-butyl-1,2,4-triphospholyl)M-(CO)$_5$] (M = Cr, W). The 1,2-shifts of the metals have activation barriers similar to those of **4**.[15] Unluckily, no explanation for this low activation energy has been given. A direct 1,2-shift seems to be unlikely, as it should be high in energy for metal atoms being bonded at such divergent σ-orbitals. In the case of copper complex **4**, however, it may be related to the specific properties of copper(I) triphospholyl compounds, as observed for **3**. Transferring the experimental results on **3** to binuclear **4**, a low activation barrier for π,σ rearrangements of the Cu−triphospholyl interaction can be assumed. This causes at least a transient localization of the ring π system, which is no longer occupied directly by the copper atom and may be utilized by the tungsten atom as an alternative electron reservoir. The formation of the σ(Cu),σ(W) complex **4a** may happen in one or two steps (Scheme 5).

If the tungsten atom of **4a** moves from its position at a phosphorus p_z orbital to the equivalent position of the neighbor P atom to form **4a′**, it may stay in constant contact with the π-electron density above the ring plane. This consideration fits better to the observed low activation energy of the whole process than a direct 1,2-shift of the tungsten atom.

Despite a crowded situation of three metal atoms around one triphospholyl ring, as indicated by the molecular structure in the solid state, even the ditungsten complex **5** is fluxional in solution. ^{31}P NMR spectra at ambient temperature exhibit only broad lines; when the sample is cooled to −80 °C, a well-resolved spectrum is observed (Figure 5).

(15) Mueller, C.; Bartsch, R.; Fischer, A.; Jones, P. G. *Polyhedron* **1993**, *12*(11), 1383−90.

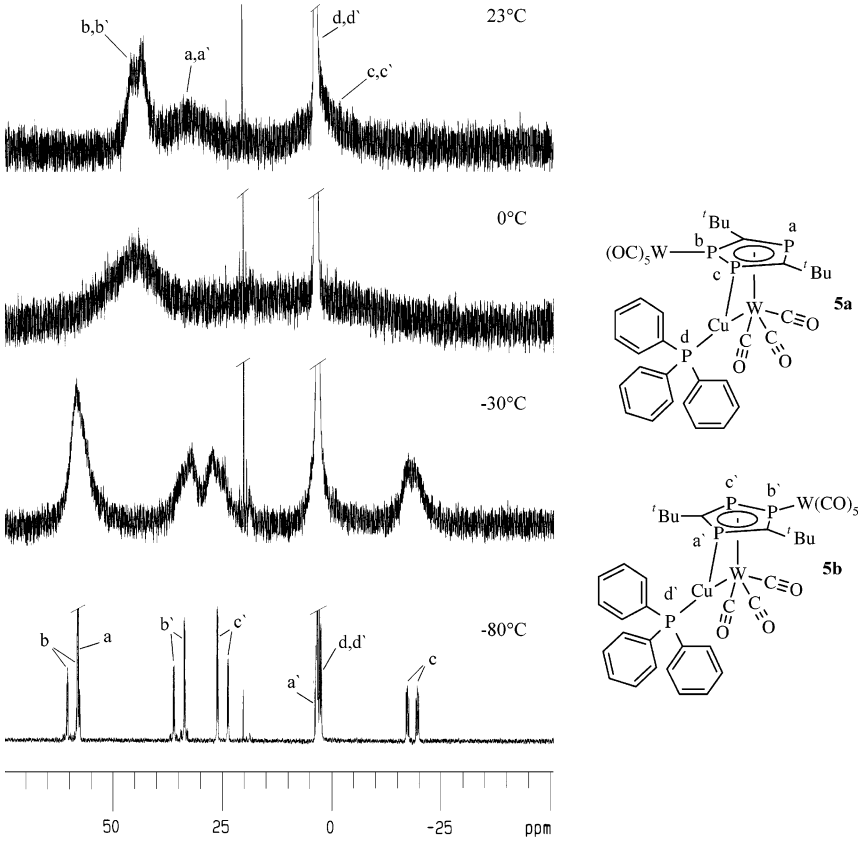

Figure 5. Variable-temperature $^{31}P\{^1H\}$ NMR spectra of **5** (161.7 MHz, CD_2Cl_2).

Scheme 5

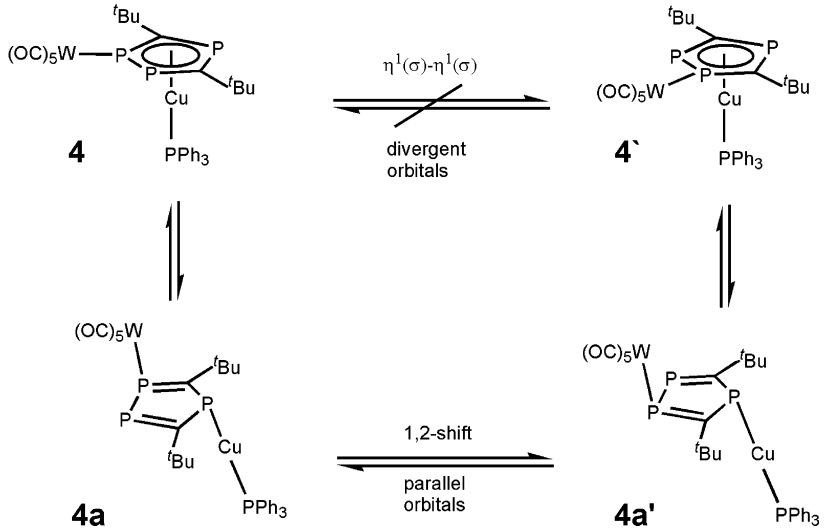

^{31}P and ^{183}W coupling patterns are completely resolved in the low-temperature $^{31}P\{^1H\}$ NMR spectrum of **5** and allow an unambiguous analysis. The spectrum consists of two sets of four signals each, which can be associated with the two isomeric compounds **5a** and **5b**. The spectrum of **5a** is in line with the bonding mode observed in the solid state, as indicated by the transoid $^2J(^{31}P_c{}^{31}P_d)$ coupling constant of 59.6 Hz. The spectrum of **5b** is closely related, but the cross metal coupling $^2J(^{31}P_a{}^{31}P_d) = 50.1$ Hz gives clear evidence for the coordination of the single ring phosphorus atom P_a to the copper atom. Connectivity and coupling constants of both isomers **5a** and **5b** are depicted in Figure 6.

5b is a unique case. All known 1,2,4-triphospholyl complexes with η^1-coordinated metal fragments bind them through one of the two adjacent phosphorus atoms. The existence of **5b** points to the fact that the general preference of the coordination toward one of the neighboring phosphorus atoms seems to be not only governed by the basicity of the lone pairs but also modified by steric effects and entropy. The available space for a metal atom which is attached to one of the lone pairs of the ring phosphorus atoms P(1) or P(2) is almost the same for **5**. As a result, both isomers should be close to isoenergetic and the concentrations of **5a** and **5b** are almost identical, due to the integration values

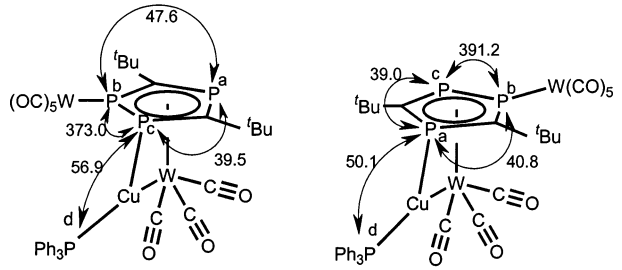

5a **5b**

Figure 6. Connectivity and ^{31}P coupling constants in Hz of **5a** and **5b** in solution.

of their ^{31}P NMR spectra at low temperature. This accidental but helpful coincidence allows the determination of the activation energy of the rearrangement process $\Delta G^{\ddagger}_{exchange} = 44(2)$ kJ/mol simply by determining the coalescence temperatures of the ^{31}P NMR signals even in the case of two different species[12] ($T_{coalescence} = 0 \pm 5$ °C for P(a) and P(c) and -10 ± 5 °C for P(b)). When it moves from P(2) to P(1), the copper atom has to pass ring carbon atom C(1). This may create a temporal bonding situation C(1)−Cu(1) with a local energetic minimum or a transition state; thus, $\Delta G^{\ddagger}_{exchange}$ can to be regarded as the upper limit for the difference in bond energy for the two cases Cu(I)−C_{ring} and Cu(I)−P_{ring} of **5**. As a result, the activation energy represents an experimental hint of the specific contribution of phosphorus atoms toward the π bonding of unsaturated P-heterocycles.

Conclusions

When the coinage metal ions Au(I) and Cu(I) are combined with the ligand 3,5-di-*tert*-butyl-1,2,4-triphospholyl, a wide variety of complexation modes are observed, ranging from monomeric η^5-π to different forms of mono- and dimeric η^1 bonding with localized and delocalized ring π-electron systems, respectively. Most of the compounds are highly fluxional, thus indicating low activation barriers between the different bonding modes which connect metal atoms and the unsaturated P-heterocyclic ligands. The features are unprecedented for the otherwise closely related cyclopentadienyl Au(I) and Cu(I) complexes. Qualitatively, the results can be rationalized by a combination of two complementary flexible building blocks. The relative small difference in energy for the Cu(I) ion in bonding situations with 18 or 16 VE and the possibility to go as far as 14-VE species gives rise to a remarkable structural manifold in copper complex chemistry. On the other hand, the 1,2,4-triphospholyl ligand not only exhibits a cyclopentadienyl-like π-electron system but also combines it with the phosphorus lone pairs, which are sources of three almost ball-shaped centers of electron density. They are thus accessible for soft Lewis acids such as Cu(I) and Au(I) not only in the plane of the ring but from the side as well. This way the lone pairs bridge the horizontal node of the π-system and give freedom to metals which are capable of utilizing the complete electron density around the ring to stabilize transition, intermediate, and even ground states outside the standard bonding situations of cyclopentadienylmetal complexes. These experimental results define some of the specific ligand properties of unsaturated P-rich phosphorus heterocycles.

Experimental Section

General Considerations. All experiments were conducted under a nitrogen atmosphere by using standard Schlenk and cannula techniques. Solvents were dried according to the described procedures and used freshly distilled from the drying agent. $[ClCu(PPh_3)]_4$ was prepared according to the literature.[16] 1-(Trimethylstannyl)-3,5-di-*tert*-butyl-1,2,4-triphosphole (**1a**) was prepared as described previously[3] and distilled under oil pump vacuum for purification. $^{31}P\{^1H\}$ NMR spectrum simulation of **5** was carried out using the program Nuts 2D Version 5.084 (NMR Data Processing Program, Acorn NMR, 1995).

[(3,5-di-*tert*-butyl-1,2,4-triphospholyl)Cu(PPh$_3$)] (3). A 0.428 g (0.296 mmol) portion of $[ClCu(PPh_3)]_4$ was dissolved in 40 mL of CH_2Cl_2, and 0.498 g (1.261 mmol) of 1-(trimethylstannyl)-3,5-di-*tert*-butyl-1,2,4-triphosphole (**1a**) in 10 mL CH_2Cl_2 was added at −40 °C. The reaction mixture was warmed to room temperature and was stirred for an additional 3 h. All volatile components of the reaction mixture were removed under oil pump vacuum. The yellow residue was dissolved in 50 mL of *n*-hexane, and the solution was filtered and concentrated under vacuum down to ca. 30 mL. **3** crystallized at −18 °C. The solid was washed twice at −60 °C with small amounts of *n*-hexane and dried in vacuo. Chromatography on SiO_2/5% H_2O with toluene as the eluent led to a luminous yellow fraction, which was recrystallized from *n*-hexane at −30 °C to yield 0.545 g (0.98 mmol, 82.6%) of **3** as a microcrystalline yellow to orange solid.

Spectroscopic Data for 3. ^1H NMR (269.7 MHz, $CDCl_3$, room temperature): δ 1.48 (s, 18H, CH_3), 7.31−7.45 (m, 15H, C_6H_5). $^{13}C\{^1H\}$ NMR (67.83 MHz, $CDCl_3$, room temperature): δ 194.14 (dpt (doublet/pseudo triplet), $^1J(^{31}P,^{13}C) = 73.7$ Hz, $\sum[^1J(^{31}P,^{13}C) + {}^2J(^{31}P,^{13}C)] = 99.2$ Hz, C_{ring}), 133.70 (d, $^2J(^{31}P,^{13}C) = 16.2$ Hz, *o*-Ph *C*), 133.17 (d, $^1J(^{31}P,^{13}C) = 26.1$ Hz, *i*-Ph *C*), 129.83 (s, *p*-Ph *C*), 128.53 (d, $^3J(^{31}P,^{13}C) = 9.3$ Hz, *m*-Ph *C*), 40.08 (dpt, $^2J(^{31}P,^{13}C) = 19.1$ Hz, $\sum[^2J(^{31}P,^{13}C) + {}^3J(^{31}P,^{13}C)] = 12.2$ Hz, $C(CH_3)_3$), 36.87 (br (broad signal), no coupling resolved, C(CH_3)$_3$). $^{13}C\{^1H\}$ NMR (100.4 MHz, [D_8]-toluene, −90 °C): δ 39.2 (br, $C(CH_3)_3$), 38.1 (br, $C(CH_3)_3$), 34.5 (br, C(CH_3)$_3$), 135−122 (Ph *C*, not assigned due to overlapping solvent signals). $^{31}P\{^1H\}$ NMR (161.7 MHz, [D_8]toluene, +48 °C): rapid exchange of isomers, [AB_2X] spin system, δ 204.08 (br, 1P, $P(A) = P_{ring}$), 187.62 (d, $^2J(^{31}P,^{31}P) = 55.0$ Hz, 2P, $P(B) = P_{ring}$), 8.24 (br, 1P, $P(X) = P(C_6H_5)_3$). $^{31}P\{^1H\}$ NMR (161.7 MHz, [D_8]toluene, −30 °C): [(η^5-*t*-$Bu_2C_2P_3$)(PPh_3)Cu] (**3a**), [AB_2X] spin system, δ 197 (br, 1P, $P(A) = P_{ring}$), 182 (br, 2P, $P(B) = P_{ring}$), 17 ((br, 1P, $P(X) = PPh_3$); [(η^1-*t*-$Bu_2C_2P_3$)-($P(C_6H_5)_3$)Cu] (rapidly interchanging isomers **3b** and **3c**), [AX_2Y] spin system, δ 275 (br, 1P, $P(A) = P_{ring}$), 176.5 (br, 2P, $P(X) = P_{ring}$), −6 (br, $P(Y) = PPh_3$). $^{31}P\{^1H\}$ NMR (161.7 MHz, [D_8]toluene, −90 °C): mixture of isomers **3b** and **3c**, [(η^1-*t*-$Bu_2C_2P_3$)(PPh_3)Cu], two independent [ABCD] spin systems, δ 290.5 (br, 1P, P(A1 or A2) = P_{ring}), 256.0 (br, 1P, P(A2 or 1) = P_{ring}), 235 (br, 1P, P(B1 or B2) = P_{ring}), 192.7 (br, d, $^1J(^{31}P$-(B),^{31}P(C)) = 357 Hz, 1P, P(B2 or B1) = P_{ring}), 168.1 (br, d, $^1J(^{31}P(B),^{31}P(C)) = 357$ Hz, 1P, P(C2 or C1) = P_{ring}), 122.3 (br, 1P, P(C1 or C2) = P_{ring}), 1.1 ((br, 1P, P(D1 or D2) = $P(C_6H_5)_3$), −3.7 ((br, 1P, P(D2 or D1) = PPh_3). MS (FD$^+$, toluene): *m*/*z* (%) 262 (100) $[PPh_3]^+$, 556 (14) [(*t*-$Bu_2C_2P_3$)(PPh_3)Cu]$^+$, 588 (5) [{PPh_3}$_2$Cu]$^+$, 884 (25) [(*t*-$Bu_2C_2P_3$)$_2$(PPh_3)Cu_2]$^+$, 1114 (1.5) [(*t*-$Bu_2C_2P_3$)$_2$ (PPh_3)$_2Cu_2$]$^+$. Mp: 142 °C.

[(μ,η(1):η(1−5)-(3,5-di-*tert*-butyl-1,2,4-triphospholyl)-{W(CO)$_5$}{Cu(PPh$_3$)}] (4) and [(μ,η(1):η(1−5):η(1)-(3,5-di-

(16) Costa, G.; Reisenhofer, E.; Stefani, L. *J. Inorg. Nucl. Chem.* **1965**, *27*, 2581−2584.

***tert*-butyl-1,2,4-triphospholyl){W(CO)$_5$}{W(CO)$_3$}{Cu(PPh$_3$)}](*W*−*Cu*) (5).** A 0.269 g (0.76 mmol) portion of W(CO)$_6$ in 120 mL of THF was irradiated for 1 h with a high-pressure mercury lamp. At −40 °C 0.311 g (0.56 mmol) of [(3,5-di-*tert*-butyl-1,2,4-triphospholyl)Cu(PPh$_3$)] (**3**) in 20 mL of THF was added. The solution was warmed to room temperature, and all volatile components of the mixture were removed under vacuum. The residue was extracted six times with 10 mL of *n*-hexane, the combined solutions were filtered, and the solvent was removed again in vacuo. The remaining solid was dissolved in a few milliliters of CH_2Cl_2 and covered with a layer of *n*-hexane. Storage for 5 days at 4 °C led to orange crystalline material. It was isolated, washed with benzene and *n*-hexane, and dried in vacuo to obtain 45 mg (0.040 mmol, 7.1%) of **5**. All liquid phases were combined, and the solvents were removed in vacuo. The orange residue was chromatographed on SiO_2/5% H_2O with a toluene/*n*-hexane mixture (1/2). The color of the first fraction was yellow to orange. After removal of the solvent the residue was redissolved in CH_2Cl_2/*n*-hexane. *n*-Hexane was added to the solution at −18 °C until crystallization of **4** started. The crystals contain **4** and CH_2Cl_2 in the ratio of ca. 5:4. A total of 174 mg (0.183 mmol, 32.7%) was isolated as yellow to orange crystals.

Spectroscopic Data for 4. ^{1}H NMR (399.65 MHz, CD_2Cl_2, 23.3 °C): δ 1.356 (s, 18H, CH_3), 7.25−7.40 (m, 15H, C$_6H_5$). ^{13}C{^{1}H} NMR (100.4 MHz, CD_2Cl_2, 23.3 °C): δ 200.91 (pt, $\sum[^2J(^{31}P,^{13}C) + {}^3J(^{31}P,^{13}C)] = 30.2$ Hz, W(CO)$_4$*C*O), 197.26 (d, $^1J(^{183}W,^{13}C) = 126.3$ Hz, W(*C*O)$_4$CO), 134.0 (d, $^2J(^{31}P,^{13}C) = 14.7$ Hz, *o*-Ph *C*), 131.28 (d, $^4J(^{31}P,^{13}C) = 1.9$ Hz, *p*-Ph *C*), 131.10 (d, $^1J(^{31}P,^{13}C) = 44.0$ Hz, *i*-Ph *C*), 129.33 (d, $^3J(^{31}P,^{13}C) = 10.9$ Hz, *m*-Ph *C*), 40.57 (dd, $^2J(^{31}P,^{13}C) = 18.3$ Hz, $^2J(^{31}P,^{13}C) = 11.0$ Hz, *C*(CH$_3$)$_3$), 36.45 (dd, $^2J(^{31}P,^{13}C) = 10.0$ Hz, $^2J(^{31}P,^{13}C) = 8.2$ Hz, C(*C*H$_3$)$_3$). ^{13}C{^{1}H} NMR (100.4 MHz, [D$_8$]toluene, −59.9 °C): δ 200.5 (d, $^2J(^{31}P,^{13}C) = 30.1$ Hz, W(CO)$_4$*C*O), 197.01 (d, $^1J(^{183}W,^{13}C) \approx 120$ Hz, W(*C*O)$_4$CO), ∼135−129 (Ph C, not assigned due to overlapping solvent signals), ∼40.1 (br, *C*(CH$_3$)$_3$), 35.96 (br, C(*C*H$_3$)$_3$). ^{31}P{^{1}H} NMR (161.7 MHz, [D$_8$]toluene, 90.0 °C): [AX$_2$Y] spin system, δ 19.10 (s, 1P, *P*Ph$_3$), 149.76 (br, 2P, P_{ring}), 198.90 (dd, $^2J(^{31}P,^{31}P) = 51.7$ Hz, 1P, P_{ring}). ^{31}P{^{1}H} NMR (161.7 MHz, CD_2Cl_2, 25.2 °C): δ 18.85 (s, 1P, *P*Ph$_3$), 127.15 (br, 1P, P_{ring}), 163.87 (br, 1P, P_{ring}), 196.86 (dd, $^2J(^{31}P,^{31}P) = 50.9$ Hz, 1P, P_{ring}). ^{31}P{^{1}H} NMR (161.7 MHz, CD_2Cl_2, −69.8 °C): [AXYZ] spin system, δ 18.69 (s, 1P, *P*Ph$_3$), 123.90 (d, $^1J(^{183}W,^{31}P) = 212.6$ Hz, dd, $^1J(^{31}P,^{31}P) = 424.5$ Hz, $^2J(^{31}P,^{31}P) = 54.2$ Hz, 1P, P_{ring}), 159.41 (ddd, $^1J(^{31}P,^{31}P) = 424.5$ Hz, $^2J(^{31}P,^{31}P) = 49.3$ Hz, $J(^{31}P,^{31}P) = 7$ Hz, 1P, P_{ring}), 192.81 (ddd, $^2J(^{31}P,^{31}P) = 54.2$ Hz, $^2J(^{31}P,^{31}P) = 49.3$ Hz, $J(^{31}P,^{31}P) = 9.7$ Hz, 1P, P_{ring}). IR (*n*-hexane/CH_2Cl_2): ν(CO) 2070 (m), 2042 (s, br), 1925 (sh) cm^{-1}. MS (FD$^+$, toluene): *m*/*z* (%) 881 (100) [M]$^+$.

Spectroscopic Data for 5.

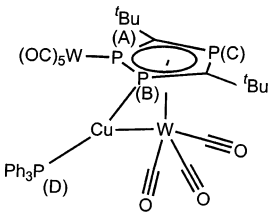

5a

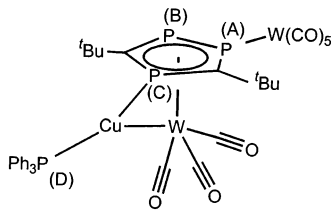

5b

^{1}H NMR (399.65 MHz, CD_2Cl_2, 22.9 °C): δ 1.07 (s, 9H, CH_3), 1.31 (s, 9H, CH_3), 7.35−7.50 (m, 15H, C$_6H_5$). ^{1}H NMR (399.65 MHz, CD_2Cl_2, −79.9 °C): δ 0.99 (s, 9H, CH_3), 1.07 (s, 9H, CH_3), 1.23 (s, 9H, CH_3), 1.40 (s, 9H, CH_3), 7.35−7.55 (m, 30H, C$_6H_5$). ^{13}C{^{1}H} NMR (100.4 MHz, CD_2Cl_2, 22.9 °C): δ 212.75 (d, $^1J(^{183}W,^{13}C) = 167.6$ Hz, W(*C*O)$_3$), 198.54 (d, $^2J(^{31}P,^{13}C) = 34.8$ Hz, W(CO)$_4$(*C*O)), 196.49 (d, $^1J(^{183}W,^{13}C) = 127.2$ Hz, d, $^2J(^{31}P,^{13}C) = 2.7$ Hz, W(*C*O)$_4$(CO)), 134.15 (d, $J(^{31}P,^{13}C) = 14.7$ Hz, *o*-Ph *C*), 131.63 (s, *p*-Ph *C*), 129.66 (d, $J(^{31}P,^{13}C) = 10.0$ Hz, *m*-Ph *C*), 129.55 (d, $^1J(^{31}P,^{13}C) = 41.2$ Hz, *i*-Ph *C*), 38.77 (dd, $^2J(^{31}P,^{13}C) = 16.0$ Hz, $^2J(^{31}P,^{13}C) = 5.0$ Hz, *C*(CH$_3$)$_3$), 38.44 (dd, $^2J(^{31}P,^{13}C) \approx 12.4$ Hz, $^2J(^{31}P,^{13}C) \approx 12.4$ Hz, *C*(CH$_3$)$_3$) 36.243 (br, C(*C*H$_3$)$_3$). ^{31}P{^{1}H} NMR (161.7 MHz, CD_2Cl_2, 23.7 °C): δ 44.5 (br, d, $^1J(^{31}P(A),^{31}P(B)) = 322$ Hz, 1P, *P*(A) = P_{ring}), 32.6 (br, 1P, *P*(C) = P_{ring}), 3.7 (br, 1P, *P*(B) = P_{ring}), 3.7 (s, 1P, *P*(D) = *P*Ph$_3$). ^{31}P{^{1}H} NMR (161.7 MHz, CD_2Cl_2, −79.9 °C): **5a**, [ABCD] spin system, δ 59.41 (d, $^1J(^{183}W,^{31}P) = 238.1$ Hz, dd, $^1J(^{31}P(A),^{31}P(B)) = 373.98$ Hz, $^2J(^{31}P(A),^{31}P(C)) = 47.66$ Hz, 1P, *P*(A) = P_{ring}), 57.96 (dd, $^2J(^{31}P(A),^{31}P(C)) = 47.66$ Hz, $^2J(^{31}P(B),^{31}P(C)) = 39.48$ Hz, 1P, *P*(C) = P_{ring}), 3.34 (d, $^2J(^{31}P(B),^{31}P(D)) = 56.95$ Hz, 1P, *P*(D) = *P*Ph$_3$), −18.37 (d, $^1J(^{183}W,^{31}P) = 18.9$ Hz, ddd, $^1J(^{31}P(A),^{31}P(B)) = 372.98$ Hz, $^2J(^{31}P(B),\ ^{31}P(C)) = 39.48$ Hz, $^2J(^{31}P(B),^{31}P(D)) = 56.95$ Hz, 1P, *P*(B) = P_{ring}); **5b**, [ABCD] spin system, δ 34.69 (d, $^1J(^{183}W,^{31}P) = 231.2$ Hz, dd, $^1J(^{31}P(A),^{31}P(B)) = 391.24$ Hz, $^2J(^{31}P(A),^{31}P(C)) = 40.81$ Hz, 1P, *P*(A) = P_{ring}), 25.05 (dd, $^1J(^{31}P(A),^{31}P(B)) = 391.24$ Hz, $^2J(^{31}P(B),^{31}P(C)) = 38.98$ Hz, 1P, *P*(B) = P_{ring}), 3.51 (d, $^1J(^{183}W,^{31}P) = 9.9$ Hz, ddd, $^2J(^{31}P(A),^{31}P(C)) = 40.81$ Hz, $^2J(^{31}P(B),^{31}P(C)) = 38.98$ Hz, $^2J(^{31}P(C),^{31}P(D)) = 50.1$ Hz, 1P, *P*(C) = P_{ring}), 2.64 (d, $^2J(^{31}P(C),^{31}P(D)) = 50.1$ Hz, 1P, *P*(D) = *P*Ph$_3$); chemical shifts and coupling constants have been obtained by iterative spectrum simulation. IR (*n*-hexane/CH_2Cl_2): ν(CO) 2075 (m), 2026 (sh), 1966 (s, br), 1945 (s, br), 1898 (m, br), 1860 (m, br), 1864 (m, br), 1824 (m, br) cm^{-1}. Raman (solid): ν(CO) 2073 (s), 1985 (s), 1953 (m), 1929 (m), 1883 (m), 1867 (m); ν(CC$_{phenyl}$) 1584 (w), ν(PP) and ν(PC) 900−1100, ν(WC) = 405−561; ν(WP) 333, 245 cm^{-1}. MS (FD$^+$, CH_2Cl_2): *m*/*z* (%) 262 (30) [PPh$_3$]$^+$, 1149 (100) [M]$^+$. Anal. Calcd for (C$_{36}$H$_{33}$CuP$_4$O$_8$W$_2$): C, 37.64; H, 2.90. Found: C, 37.81; H, 3.05. Mp: 171 °C.

Crystal Structure Determination of 4 and 5. Intensity data of **4** were collected on a Nicolet R3m/V (ω scan, 5.0°/min, Mo Kα radiation, graphite monochromator, $\lambda = 0.710\ 73$ Å) using the P3/PC software.[17] Intensity data of **5** were collected on a Siemens P4 diffractometer (ω scan, 4.0°/min, Mo Kα radiation, graphite monochromator, $\lambda = 0.710\ 73$ Å) using the XSCANS 2.20 software.[18] The structures were solved by direct methods and refined by full-matrix least-squares procedures against F^2 with all reflections using SHELXTL programs.[19] All non-hydrogen atoms were refined anisotropically. The hydrogen atoms are geometrically positioned. Crystal data and experimental details are listed in Table 3. All significant residual electron density maxima are in close vicinity of the tungsten atoms and might be due to an insufficient absorption correction or break-off effects.

Acknowledgment. This work was supported by the Deutsche Forschungsgemeinschaft and the Fonds der Chemischen Industrie. M.Z. is grateful for a scholarship by the DFG-Graduiertenkolleg Phosphorchemie als Bindeglied verschiedener chemischer Disziplinen, at the University of Kaiserslautern, Kaiserslautern, Germany. We also thank Dr. M. Moll for the measurement of variable-temperature NMR spectra.

Supporting Information Available: Further details of the structure determination, including tables of atomic coordinates, bond distances and angles, and thermal parameters. This material is available free of charge via the Internet at http://pubs.acs.org.

OM030570I

(17) Siemens Analytical X-ray Instruments Inc., Madison, WI, 1989.
(18) XSCANS 2.20; Siemens Analytical X-ray Instruments Inc., Madison, WI, 1996.
(19) Sheldrick, G. M. SHELXTL NT V5.1; Bruker AXS, Madison, WI, 1999.